

A retroviral mutagenesis screen reveals strong cooperation between *Bcl11a* overexpression and loss of the *Nf1* tumor suppressor gene

Bin Yin,¹ Ruud Delwel,² Peter J. Valk,² Margaret R. Wallace,³ Mignon L. Loh,⁴ Kevin M. Shannon,⁴ and David A. Largaespada¹

¹Masonic Cancer Center and Department of Genetics, Cell Biology and Development, University of Minnesota, Minneapolis; ²Department of Hematology, Erasmus University Medical Centre, Rotterdam, The Netherlands; ³Department of Molecular Genetics and Microbiology, Center for Mammalian Genetics, University of Florida College of Medicine, Gainesville; and ⁴Department of Pediatrics, University of California, San Francisco

NF1 inactivation occurs in specific human cancers, including juvenile myelomonocytic leukemia, an aggressive myeloproliferative disorder of childhood. However, evidence suggests that *Nf1* loss alone does not cause leukemia. We therefore hypothesized that inactivation of the *Nf1* tumor suppressor gene requires cooperating mutations to cause acute leukemia. To search for candidate genes that cooperate with *Nf1* deficiency in leukemogenesis, we performed a forward genetic screen using retroviral insertion mutagen-

esis in *Nf1* mutant mice. We identified 43 common proviral insertion sites that contain candidate genes involved in leukemogenesis. One of these genes, *Bcl11a*, confers a growth advantage in cultured *Nf1* mutant hematopoietic cells and causes early onset of leukemia of either myeloid or lymphoid lineage in mice when expressed in *Nf1*-deficient bone marrow. *Bcl11a*-expressing cells display compromised p21^{Cip1} induction, suggesting that *Bcl11a*'s oncogenic effects are mediated, in part, through suppression of p21^{Cip1}.

Importantly, *Bcl11a* is expressed in human chronic myelomonocytic leukemia and juvenile myelomonocytic leukemia samples. A subset of AML patients, who had poor outcomes, of 16 clusters, displayed high levels of *BCL11A* in leukemic cells. These findings suggest that deregulated *Bcl11a* cooperates with *Nf1* in leukemogenesis, and a therapeutic strategy targeting the *BCL11A* pathway may prove beneficial in the treatment of leukemia. (Blood. 2009;113:1075-1085)

Introduction

Neurofibromatosis type 1 syndrome (NF1) is an inherited disease caused by germline mutations of the NF1 gene.¹ NF1 encodes neurofibromin, a GTPase-activating protein that negatively regulates N-, H-, K-, and R-RAS signaling.² Loss of NF1 function results in elevated Ras-GTP levels in neoplastic cells of patients with NF1.^{3,4} Thus, NF1 deficiency has been proposed to be functionally equivalent to activation of a RAS oncogene. Neurofibromin may have additional roles in growth control.⁵⁻⁸ Thus, further investigations into pathways altered in NF1-associated malignancies may shed light on these mechanisms.

Children with NF1 syndrome show a markedly increased incidence of myeloid malignancies, particularly juvenile myelomonocytic leukemia (JMML), which can further progress into acute myeloid leukemia (AML).⁹ Similarly, mice with a germline *Nf1* mutation manifest some phenotypes of NF1 disease and thus provide a tractable model for investigating NF1-associated complications.¹⁰ Notably, evolution to AML is not observed in mice bearing mutant *Nf1* alone. Instead, murine data from competitive repopulation experiments¹¹ and the long latency of myeloid disease observed in recipients transplanted with *Nf1*^{-/-} fetal liver cells¹² support the possibility that a *Nf1*^{-/-} leukemia-initiating cell must acquire one or more additional mutations to cause leukemia. However, little is known about the nature of these genetic abnormalities. We therefore set out to identify genetic events cooperating with inactivation of *Nf1* in leukemogenesis.

The B-cell leukemia 11A gene (*BCL11A/Evi9/CTIP1*) is essential for normal lymphoid development¹³ and has been associated with hematologic malignancies.^{14,15} The *BCL11A* gene was initially identified from aberrant chromosomal translocations involving the immunoglobulin heavy chain locus detected in B-cell non-Hodgkin lymphomas.¹⁴ It encodes a Krüppel-like zinc-finger protein containing 3 C2H2 zinc finger motifs, a proline-rich region, and an acidic domain. *BCL11A* functions as a transcriptional regulator via directly binding to a guanine cytosine (GC)-rich DNA motif. *BCL11A* is expressed predominantly in brain, spleen, and testis and is down-regulated in a leukemia cell line under induction of myeloid differentiation.¹⁶

BXH-2 mice have proven to be a powerful model system to identify genetic lesions causally associated with leukemia.¹⁷ Approximately 15% of BXH-2 myeloid leukemias have proviral insertions at ecotropic viral integration site 2 (*Evi2*), all of which are located within a single large intron of the *Nf1* gene.¹⁸ Consequently, *Nf1* gene function is disrupted, and no wild-type gene product could be detected in *Evi2*-bearing leukemias.¹⁹ These studies support the idea that BXH-2 AML is an excellent system to explore the mechanisms of *Nf1*-associated leukemia.

We performed a genetic screen in the BXH-2 AML model using retroviral insertion mutagenesis to search for cooperating genetic events in *Nf1*-associated myeloid leukemia. Here we report isolation of 43 common insertion sites (CISs). One such CIS, *Evi9*, is

Submitted March 11, 2008; accepted October 14, 2008. Prepublished online as Blood First Edition paper, October 23, 2008; DOI 10.1182/blood-2008-03-144436.

The publication costs of this article were defrayed in part by page charge payment. Therefore, and solely to indicate this fact, this article is hereby marked "advertisement" in accordance with 18 USC section 1734.

The online version of this article contains a data supplement.

© 2009 by The American Society of Hematology

associated with *Nfl*-deficient BXH-2 AML and targets *Bcl11a*. We found that overexpression of *Bcl11a* causes leukemia in mice under the condition of *Nfl* deficiency. *Bcl11a* also promotes cell growth and suppresses p21^{Cip1} induction. High expression levels of *Bcl11a* are seen in certain subsets of AML patients.

Methods

Cell culture and mice

The *Nfl*-deficient and *Nfl*-proficient mouse hematopoietic cells immortalized with RED-Myb were maintained in the ASM media.^{12,20,21} The 293T were purchased from the ATCC (Manassas, VA) and maintained in Dulbecco modified Eagle medium (DMEM), supplemented with heat-inactivated 10% fetal bovine serum and 1% penicillin/streptomycin. Cell counts were determined manually using a hemocytometer (Reichert, Buffalo, NY). For all the studies described herein, cells growing in the logarithmic phase of growth were used. The *Nfl*^(flox/+) and *Nfl*^(Fcr/+) mouse lines have been previously described.^{22,23} The C57BL/6J and C57BL/6J.BoyJ strain of mouse was purchased from the National Cancer Institute (Bethesda, MD). Mice were housed, bred, and manipulated under specific pathogen-free conditions, following the University of Minnesota's regulations on institutional animal care for research use.

Patient samples

The JMML and chronic myelomonocytic leukemia patient samples used in this study were obtained following protocols approved by the University of Minnesota Internal Review Board, with informed consent obtained in accordance with the Declaration of Helsinki.

Isolation of proviral integration sites

A total of 2 μ g genomic DNA was digested overnight with the combination of restriction enzymes *TaqI*, *BspLU11I*, and *BclI* (Roche Diagnostics, Indianapolis, IN), and subjected to the STA-polymerase chain reaction (PCR) and SplinkBlunt-PCR protocol, as previously reported.²⁴ After electrophoresis on 1.2% of agarose gel, individual secondary PCR bands were cloned into TOPO TA vector (Invitrogen, Carlsbad, CA) for sequencing.

Sequence analysis

Proviral insertion sites (PISs) were mapped by searching against Ensembl and Celera Mouse Genome Database using the BLASTN algorithm.²⁵

RT-PCR

Total RNA was extracted from tumor samples using TRIzol (Invitrogen), followed by treatment with DNase I, according to the manufacturer's instructions. Reverse-transcription PCR (RT-PCR) was conducted using the SuperScript II First Strand cDNA Synthesis system (Invitrogen), followed by PCR using gene-specific primers, as reported previously.²⁰ Sequences of primers used in the RT-PCR for amplification of genes examined in this study are available on request.

Southern blotting analysis

A total of 10 μ g genomic DNA was digested with the indicated restriction enzymes and resolved on a 1.0% agarose gel, followed by standard blotting, hybridization, and radioautography procedure.²⁰ The pMIGR-Bcl11a construct-specific probe and the cDNA probe specific for the *Ing1* gene were labeled with α -³²P-dCTP using the random priming labeling approach.²⁰

Construction of pMIGR-Bcl11a, retrovirus production, and establishment of stable transductants

Bcl11a cDNA (a gift from Dr Takuro Nakamura, The Cancer Institute, Japanese Foundation for Cancer Research, Tokyo, Japan) was fused with His tag by PCR and subcloned into the *BglII-XhoI* site of a retroviral

expression vector, pMIGR (a gift from Dr Juli Miller, The University of Pennsylvania, Philadelphia, PA), to create pMIGR-Bcl11a, which expresses both *Bcl11a* and enhanced green fluorescence protein (EGFP).²⁶ Constructs were verified by sequencing. pMIGR-Bcl11a and empty vector were used to transfect 293T cells for production of vesicular stomatitis virus G (VSV-G) pseudotyped retrovirus, as previously described.²⁶ The retrovirus was used to infect cultured cells in the presence of 4 μ g/mL polybrene. The EGFP-positive cells were sorted from the population of transduced cells by flow cytometry (BD Biosciences, San Jose, CA).

Bone marrow transduction and transplantation assay

Bone marrow cells were harvested from donor mice 5 days after they were treated with 150 mg/kg 5-fluorouracil, as described previously.²⁷ Cells were stimulated for 24 hours with interleukin-6 (IL-6), IL-3, and stem cell factor (SCF) before being infected with the indicated viruses in the presence of 2 μ g/mL polybrene. Transduced bone marrow cells were intravenously injected into lethally irradiated C57BL/6J.BoyJ mice at 10⁶ cells per recipient mouse. Mice were observed on a daily basis for any signs of disease.

Immunologic phenotyping and flow cytometry

As previously described,²⁸ cells were incubated on ice in blocking buffer containing CD16/32 Fc blocker for 15 minutes, before staining with antibodies on ice for 25 minutes. Subsequently, cells were washed and subjected to flow cytometry analysis using 4-color FACSCalibur flow cytometer (BD Biosciences) following the manufacturer's instruction. All fluorochrome-conjugated antibodies were purchased from BD PharMingen (San Diego, CA), and the applied dilutions of antibodies were optimized in our laboratory. CD45.1-phycoerythrin (PE) and CD45.2-fluorescein isothiocyanate (FITC) were used to distinguish donor and recipient cellular origin. Conjugated antibodies staining for Mac-1, Gr-1, T-cell receptor β (TCR- β), and B220 were used to examine the origin of cell lineages. Data were analyzed using FlowJo 7.0 Software (TreeStar, Ashland, OR).

Cell growth assay

A total of 10⁵ cells per well were seeded into 24-well plates in quadruplicate in acid sphingomyelinase medium¹⁹ complemented with 10% WEHI-3-conditioned medium, and cultured at 37°C in a 10% CO₂ humidified incubator. An aliquot of 10 μ L homogeneous cell suspensions was taken at 0, 24, and 48 hours, respectively, to count the cumulative cell number.

Western blot

Cells were washed with phosphate-buffered saline (PBS) and lysed in Nonidet P-40 (NP-40) lysing buffer.²¹ Protein concentrations were determined using the Bradford method (Pierce Chemical, Rockford, IL). A total of 40 μ g total protein was boiled for 5 minutes before electrophoresis on 10% sodium dodecyl sulfate-polyacrylamide gel electrophoresis (SDS-PAGE) gels, and subsequently blotted to methanol-activated polyvinylidene difluoride (PVDF) membrane (Bio-Rad, Hercules, CA). The blots were blocked and incubated with the primary antibodies as follows: His probe (1:2000; Santa Cruz Biotechnology, Santa Cruz, CA), rabbit anti-extracellular signal-regulated kinase 1 (ERK1; 1:1500; Santa Cruz Biotechnology), and mouse antibodies against indicated cell-cycle regulatory proteins are available in the Cell Cycle I/II Sampler Kit (BD PharMingen). After incubation with horseradish peroxidase (HRP)-conjugated secondary antibodies, blots were developed by the enhanced chemiluminescence detection system (GE Healthcare, Little Chalfont, United Kingdom) and then exposed to the X-ray films.

Statistics

Student *t* tests were used to compare means of cell number between different genotypes of immortalized hematopoietic cells. The Fisher exact test was applied to determine whether there was difference in incidence of *Bcl11a*-targeting PIS between leukemia with wild-type *Nfl* and *Nfl* deficiency. Differences between groups were considered significant at values of *P* less than .05.

Results

Identification of CISs of BXH-2 MuLV

We examined genomic DNA specimens derived from BXH-2 strain AML, which are *Nf1*-intact ($n = 25$) or *Nf1*-deficient ($n = 55$). In 19 *Nf1*-deficient AMLs, the *Nf1* gene was disrupted by murine leukemia virus (MuLV) insertions within the *Evi2* locus,^{12,29} and 36 AMLs were generated using *Nf1* knockout mice (Figure 1).^{12,29} Somatic proviral insertions in these AML were isolated efficiently with STA-PCR and SplinkBlunt-PCR that we have developed.²⁴ We obtained 197 informative PISs, with 2.46 PISs recovered from each tumor on average (Table S1, available on the *Blood* website; see the Supplemental Materials link at the top of the online article). We expect that this is close to full PIS recovery compared with the number of PISs per BXH-2 tumor detected by Southern blotting assay (data not shown).^{24,29}

Mapping of these PISs using the Ensembl mouse genome database uncovered 12 CISs, including 9 novel CISs (group I CIS in Table 1) and 3 previously reported CISs (group II CIS in Table 1). For some PISs isolated only once in this screen, cross-reference to other PIS profiles deposited in the Retrovirus Tagged Cancer Gene Database (<http://rtcgdb.abcc.ncifcrf.gov/>) resulted in the recognition of 13 CISs (group IV CIS in Table 1). Similarly, 17 CISs were identified where our single PISs hit known CISs (group V CIS in Table 1). Interestingly, many CISs mapped to chromosomal locations that are syntenic to sites of recurrent structural abnormalities in human malignancies (Table S2).

To explore the biologic significance of the 40 new and known CIS-associated genes (Table 1), the Ingenuity Pathway Analysis program (<http://www.ingenuity.com/>) was used to produce molecular networks. The NF- κ B pathway was predicted with the highest likelihood, organizing 14 (or 39%) of the total genes found in our study. The second most probable pathway involved 9 candidate genes, including *Bcl11a*. These data suggest that dysregulation of the NF- κ B pathway and *Bcl11a*-associated pathway may contribute to the development of AML.

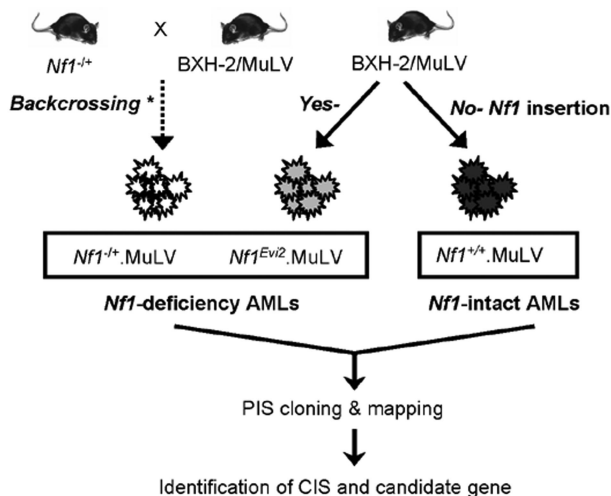


Figure 1. Strategy for collection of leukemia with intact or deficient *Nf1* gene for this study. *Nf1*^{+/+}.MuLV indicates MuLV-infected *Nf1*-intact leukemia; *Nf1*^{-/-}.MuLV, MuLV-infected leukemia with engineered null *Nf1* allele. *Nf1*^{Evi2}.MuLV, MuLV-infected leukemia with *Nf1* disruption by proviral insertion into *Nf1*. * indicates that the leukemias were produced previously by the laboratory of Dr Camy I. Brannan (deceased) through multiple rounds of backcrossing *Nf1*-null mice onto the BXH-2 strain of mice.^{12,29} PIS indicates proviral insertion site; and CIS, common proviral insertion site.

Analysis of candidate leukemia genes

The *Ahi1/Myb* CIS represents the most frequent insertion site in our screen. Fourteen proviral insertions with either orientation were recovered immediately downstream to the *Ahi-1* gene, also approximately 35 kb downstream to *c-Myb* (Figure S1), presumably enhancing transcription of *Ahi-1* and *c-Myb*. This finding highlights the potential role of deregulation of *Ahi-1* and *c-Myb* in leukemogenesis.

Bcl11a and *Spred2* were hit as often as *Meis1* and *Hoxa7/a9*, which have been strongly implicated in human myeloid leukemogenesis.³⁰ Whereas we observed a similar pattern of insertions in *Nf1*-deficient and *Nf1*-intact leukemias at most CISs, the PISs targeting *Bcl11a* and *Spred2* were all isolated from *Nf1*-deficient AMLs (Table 1). Five PISs with sense or antisense orientation were isolated from the first intron of *Spred2*, indicating that disruption of normal transcription of *Spred2* could cooperate with *Nf1* deficiency during formation of leukemia (Figure S2). Consistent with this possibility, *SPRED2* are thought to be a negative regulator of RAS/ERK signal transduction,³¹ and expression of *SPRED2* is decreased in some cancers.

To further explore the putative association between *Nf1* deficiency and *Bcl11a*-targeting insertions, which turn out to overlap with known *Evi9* insertions, Southern blot analysis of 40 additional *Nf1* intact BXH-2 AMLs with a *Bcl11a*-specific probe were performed, and we did not detect any evidence of proviral insertions ($P < .02$; Figure S5). These data suggest that *Evi9* insertions are enriched in the *Nf1*-deficient versus *Nf1*-intact AML we studied, although they are probably not unique to *Nf1* deficiency. In addition to *Bcl11a*, 3 other genes flanking *Evi9* were predicted, tentatively designated as *Evi9-PG1*, *Evi9-PG2*, and *Evi9-PG3*, respectively (<http://www.ensembl.org/>) (Figure 2A). Strikingly, unlike the majority of reported CISs, our *Bcl11a*-targeting insertions contain 5 PISs located within a narrow chromosomal region of less than 1 kb, underlining a strong correlation between insertions at *Evi9* with leukemogenesis.

To uncover the gene(s) that is the potential biologic target of proviral insertions at *Evi9*, we examined expression levels in BXH-2 leukemia of surrounding genes by RT-PCR using gene-specific primers. We could not detect any transcripts from *Evi9-PG1* and *Evi9-PG3* in these tumors (Figure 2B). *Evi9-PG2* is expressed at a higher level in the *Evi9* insertion-bearing leukemia than others. Further analysis showed that *Evi9-PG2* was only 523 bp in size, harboring a single exon without a predictable coding frame. Thus, *Evi9-PG2* could be a pseudogene, or possibly, a noncoding RNA gene. *Bcl11a* expression could be observed at different levels in 5 of 6 tumors. Sequencing confirmed the specificity of the upper RT-PCR bands shown in Figure 2B (data not shown). As expected, the highest expression level of *Bcl11a* was detected in the *Evi9* insertion-bearing leukemia only for which RNA was available, suggesting that *Bcl11a* is up-regulated as a consequence of *Evi9* insertions.

Expression of *Bcl11a* in *Nf1*-deficient bone marrow cells leads to leukemia

Our findings that (1) *Evi9* is a frequent target by MuLV, (2) *Evi9* occupies an exceptionally narrow window, (3) *Evi9* is enriched in *Nf1*-deficient tumor panel, and (4) *Bcl11a* appears to be the primary target of *Evi9* established *Bcl11a* as a strong candidate for cooperation with *Nf1* inactivation. In addition, *Bcl11a* has been implicated in the development of human lymphocytic leukemia.^{14,15,30} Therefore, we decided to investigate the role of *Bcl11a*

Table 1. Candidate leukemia genes identified in this MuLV screen

CIS group*/Gene hit†	Annotation	Tumor panel‡		
		<i>Nf1</i> ⁺	<i>Evi2</i>	<i>Nf1</i> ⁻
I				
<i>Edg3</i>	Endothelial differentiation, sphingolipid G protein-coupled receptor, 3	0	1	1
<i>ENS#1</i>	Unknown	2	1	1
<i>FLJ20186</i>	Differentially expressed in FDCCP 8	1	0	2
<i>Ing1</i>	Inhibitor of growth protein 1	1	1	1
<i>Etnk1</i>	Ethanolamine kinase 1	1	0	1
II				
<i>Bcl11a</i>	B-cell CLL/lymphoma 11A	0	3	2
<i>Spred2</i>	Sprouty protein with EVH-1 domain 2, related sequence	0	1	4
<i>Pmaip1</i>	Phorbol-12-myristate-13-acetate-induced protein 1	1	1	0
<i>Jund1</i>	Jun proto-oncogene-related gene d1	1	0	1
III				
<i>Ahi1/Myb</i>	WD domain and SH3 domain-containing gene	6	4	4
<i>Hoxa7/a9</i>	Homeobox A7/A9	2	0	2
<i>Meis1</i>	Myeloid ecotropic viral integration site 1	3	0	2
IV				
<i>Usp21</i>	Ubiquitin-specific protease 21	1	0	0
<i>Enah</i>	Enabled homolog	1	0	0
<i>Tlr2</i>	Toll-like receptor 2	1	0	0
<i>Btbe3</i>	Basic transcription element-binding protein 3	0	1	0
<i>Sar1a</i>	GTP-binding protein Sar1a	1	0	0
<i>Fgd3</i>	Facio-genital dysplasia homolog 3	1	0	0
<i>Pilrb</i>	Paired immunoglobulin-like type 2 receptor beta	0	0	1
<i>Foxd1</i>	Forkhead box protein D1	0	1	0
<i>Gata2</i>	GATA-binding protein 2	1	0	0
<i>Olig2</i>	Oligodendrocyte transcription factor 2	1	0	0
<i>Wnt7a</i>	Wingless-type MMTV integration site family, member 7A	1	0	0
<i>Ly86</i>	Lymphocyte antigen 86	0	1	0
<i>ENS#2</i>	Unknown	0	0	1
V				
<i>ENS#3</i>	Similar to eosinophil chemotactic cytokine	0	1	0
<i>Nfkb1</i>	Nuclear factor NF- κ -B p105 subunit	1	0	0
<i>Centg3</i>	Centaurin, gamma 3	1	0	0
<i>Dyrk1b</i>	Dual-specificity tyrosine-(Y) phosphorylation-regulated kinase 1b	1	0	0
<i>Tbx21</i>	T cell-specific T-box transcription factor T-bet	0	1	0
<i>Lyl1</i>	Lymphoblastic leukemia	1	0	0
<i>Cbfa2t3h</i>	Core-binding factor, runt domain, alpha subunit 2	1	0	0
<i>PHF5A</i>	PHD finger protein 5A	0	0	1
<i>Runx1</i>	Runt-related transcription factor 1	0	1	0
<i>Tcirg1</i>	T-cell, immune regulator 1	0	1	0
<i>Lin28</i>	RNA-binding protein LIN-28	0	0	1
<i>Emid2</i>	EMI domain-containing protein 2	0	0	1
<i>ATP5G2</i>	ATP synthase, H ⁺ transporting, mitochondrial complex, subunit C2	0	1	0
<i>Ifngr1</i>	Interferon- γ receptor 1	0	0	1
<i>Atp5g2</i>	ATP synthase lipid-binding protein, mitochondrial precursor	0	0	1
<i>Vegfb</i>	Vascular endothelial growth factor B	0	0	1
<i>Lmo2</i>	LIM domain only 2	1	0	0
<i>Akt1</i>	v-akt murine thymoma viral oncogene homolog 1	0	1	0

*CIS group indicates the way CISs were identified for the corresponding genes. CISs that are composed of at least 2 insertions positioned within 20-kb pairs isolated in this study, and no insertions (I), single insertions (II), or known CISs (III) have previously been reported. IV and V indicate single insertions isolated in this study for which known single insertions (IV) or CISs (V) can be found.

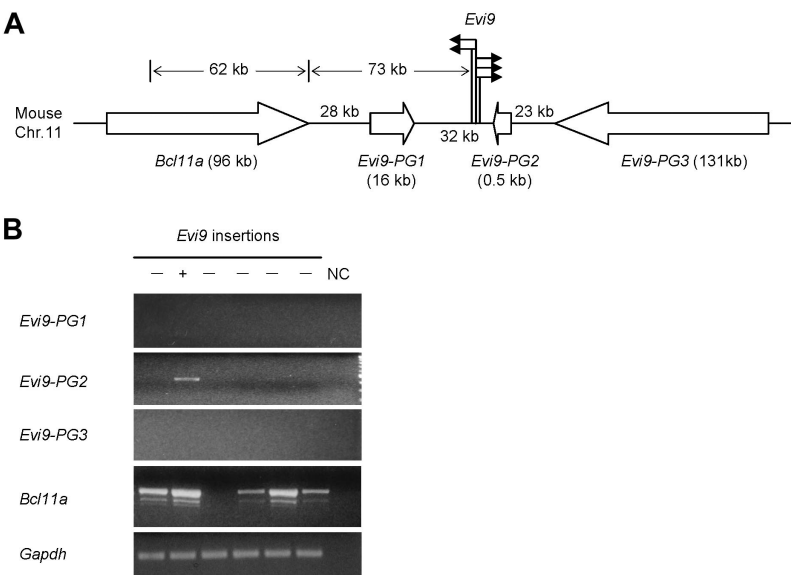
†Gene hits indicate genes located nearby CISs, which were determined according to the annotation for the mouse genome (<http://www.ensembl.org>). *ENS#1* indicates *ENSMUSG00000019986*; *ENS#2*, *ENSMUSG00000030553*; and *ENS#3*, *ENSMUSG00000010135*.

‡Tumor panel denotes the genotype of leukemia from which the corresponding proviral insertions were recovered. *Nf1*⁺ indicates tumors with intact *Nf1* alleles; *Evi2*, tumors with *Nf1* alleles disrupted by *Evi2* insertion; and *Nf1*⁻, tumors with engineered null *Nf1* allele. Values are the number of insertions isolated from each genotype of leukemia.

in leukemogenesis using the bone marrow transduction and transplantation assay (BMTT; Figure 3A).²⁷ Donor bone marrow cells were collected from C57BL/6 mice generated via a cross between mice carrying a conditional mutant (floxed) allele of *Nf1* and heterozygous *Nf1*-null (*Nf1*^{Fcr/+}) mice also transgenic for a Cre transgene driven by the *Mx-1* promoter.³² Bone marrow from wild-type *Nf1* (*Nf1*^{+/+}) C57BL/6 mice carrying the Mx1-Cre

transgene were used as a control. Wild-type and *Nf1* mutant bone marrow cells were transduced with either *Bcl11a*-expressing or empty vector VSV-G-pseudotyped retrovirus, followed by transplantation into lethally irradiated C57BL/6.BoyJ recipient mice carrying the CD45.1 allele of the cell-surface marker CD45. This allowed us to distinguish the origin of cells in transplant recipients. Therefore, 4 groups of mice were obtained, including mice

Figure 2. Analysis of *Bcl11a*-targeting CIS. (A) The schematic representation of the CIS-targeting *Bcl11a*. The solid arrows indicate the relative position and orientation of isolated proviral insertions at *Evi9*; the open arrows indicate the relative position and transcriptional orientation of *Bcl11a* and 3 other predicted genes; bracketed numbers, size (in kb) of genes. (B) Expression in BXH-2 leukemia of *Bcl11a* and 3 other predicted genes nearby *Evi9* locus (*Evi9-PG1*, *Evi9-PG2*, and *Evi9-PG3*) was detected by RT-PCR using gene-specific primers. The lanes marked “–” indicate AML samples with no *Evi9* insertions; the lane marked “+” indicates 1 of the 5 AML samples with *Evi9* insertions. *Gapdh* was used as a loading control. NC indicates water in place of cDNA as the template for PCR was set up as negative controls.



receiving *Nf1*-sufficient bone marrow cells, which had been transduced with empty vector packaged retrovirus (*Nf1*^(+/+).EV), *Nf1*-sufficient bone marrow cells transduced with *Bcl11a*-expressing retrovirus (*Nf1*^(+/+).*Bcl11a*), *Nf1*-deficient bone marrow cells transduced with empty vector packaged retrovirus (*Nf1*^(Flox/Fcr).EV), and *Nf1*-engineered bone marrow cells transduced with *Bcl11a*-expressing retrovirus (*Nf1*^(Flox/Fcr).*Bcl11a*). We administered polyI:polyC to all mice receiving these donor marrow cells to induce recombination-mediated deletion of the floxed allele by activating the Mx1-Cre transgene.³²

Approximately 3 weeks after polyI:polyC treatment, engraftment of donor cells was examined by performing PCR on genomic DNA from peripheral blood cells collected retro-orbitally from recipient mice. Primers specific to the floxed allele of *Nf1* were used (Figure S3A). The “WT” PCR band can be amplified from peripheral blood cells with all 4 genotypes, whereas the floxed *Nf1* allele-specific (“Flox”) and recombined *Nf1* allele-specific (“Del”) products can only be seen in peripheral blood cells derived from the *Nf1*^(Flox/Fcr).EV or *Nf1*^(Flox/Fcr).*Bcl11a* group of mice, indicating not only engraftment of donor bone marrow but also the occurrence of recombination of the floxed *Nf1* allele after polyI:polyC induction. The presence of residual floxed allele may reflect incomplete *Nf1* deletion mediated by polyI:polyC-induced Cre expression. Furthermore, with Fcr-null allele-specific primers, the “Fcr” band can be observed in peripheral blood cells from mice receiving *Nf1*^(Flox/Fcr).Cre bone marrow, but not from mice receiving *Nf1*^(+/+).Cre cells (Figure S3), which confirms both engraftment of donor cells and the expected genotype of bone marrow cells received. Importantly, we were able to detect the *Bcl11a*-expressing retroviral vector that was used for transduction in blood cells from the *Nf1*^(Flox/Fcr).*Bcl11a* group of mice (Figure S3C), demonstrating successful retroviral delivery of *Bcl11a* into recipient mice. These results suggest that bone marrow engraftment, recombination-mediated deletion of *Nf1*, and *Bcl11a* delivery into recipient mice had been achieved.

By 9 months after polyI:polyC induction, none of 10 mice of the *Nf1*^(+/+).EV group had become sick (Figure 3B). Two mice each had died in the *Nf1*^(+/+).*Bcl11a* ($n = 11$) and *Nf1*^(Flox/Fcr).EV ($n = 12$) cohorts (Figure 3B). By contrast, all 11 recipients that received *Nf1*^(Flox/Fcr) cells transduced with the *Bcl11a* virus became moribund by 7 months after polyI:polyC treatment, with a median latency of

107.8 days (Figure 3B). A similar trend in latency of disease was observed in an independent BMTT assay (data not shown). Most sick *Nf1*^(Flox/Fcr).*Bcl11a* mice had enlarged lymph nodes, liver, and spleen (Table S4A). Visible metastases to the liver and kidney were readily observed. Enlarged thymi were seen in 2 mice without apparent abnormalities in other organs (Table S4A). Most mice exhibited high white blood cell counts (Table S4B). Generally, there was a decrease in the levels of hemoglobin and in the number of red blood cells and platelets (Table S4B). Pathologic analysis showed an increase in the number of immature myeloid or lymphoid cells in peripheral blood and bone marrow of *Nf1*^(Flox/Fcr).*Bcl11a* mice. Spleen touch preps also displayed an excessive infiltration of blast-like cells. Significantly, neoplastic blast cells were found in multiple tissues, including bone marrow, spleen, lymph node, liver, kidney, and thymus (Figure 3C), indicating that normal tissue structures are effaced and replaced by infiltrating tumor cells. In addition, a 3.7-kb band can be detected in the enlarged lymph nodes and thymi by Southern blotting assay using a construct-specific probe (Figure S4), indicating the presence of the *Bcl11a*-expressing construct in the affected tissues. Furthermore, tumor cells isolated from 3 *Nf1*^(Flox/Fcr).*Bcl11a* mice were intravenously injected into 9 syngeneic C57BL/6J mice at 10⁶ cells per mouse, 3 mice for each tumor. The recipient mice became moribund within 6 to 10 weeks after inoculation of tumor cells, with an apparent increase in white blood cell counts similar to what has been observed in *Nf1*^(Flox/Fcr).*Bcl11a* mice, which demonstrates the transplantability of the disease developed in the BMTT assay. Together, these data show that transplantation of *Nf1*-deficient bone marrow cells overexpressing *Bcl11a* results in aggressive hematologic malignancies in recipient mice.

***Bcl11a*-overexpressing, *Nf1*-deficient leukemia is of myeloid or lymphoid lineage and derived from transduced donor cells**

The origin of the tumor cells was determined by immunostaining assay using antibodies specific for CD45.1 or CD45.2. The majority of cells isolated from enlarged lymph node, spleen, and thymus stained positive for CD45.2 (Figure 3D), indicating that these tumor cells are primarily derived from transplanted donor bone marrow. The cell lineage of origin of the leukemia was

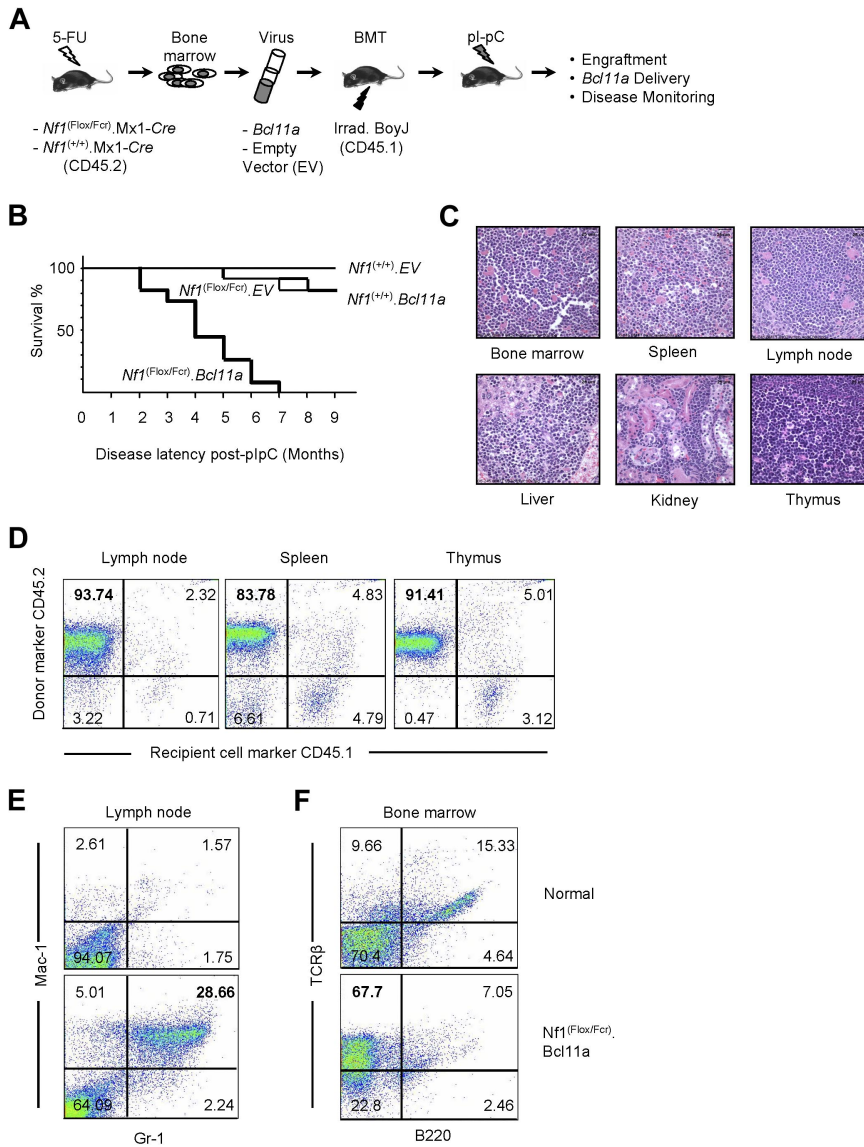


Figure 3. Examination of oncogenic effect of *Bcl11a* overexpression using the BMTT assay in mice.

(A) The BMTT scheme used in this study. (B) Survival analysis on the BMTT-recipient mice, which received *Bcl11a*- or empty vector (used as a negative control)-transduced *Nf1*-intact ("*Nf1*^(+/+).EV" and "*Nf1*^(+/+).*Bcl11a*") or *Nf1*-deficient bone marrow cells ("*Nf1*^(Flox/Fcr).EV" and "*Nf1*^(Flox/Fcr).*Bcl11a*"). (C) Histopathologic examination of the *Bcl11a*-induced leukemia in the recipient mice. Hematoxylin and eosin staining. Representative images with magnification of 60-fold are shown here. Bars represent 25 μ m. Slides were viewed with a Nikon Eclipse E600 bright light microscope (Nikon, Tokyo, Japan) using a Nikon Plan Fluor 40 \times /0.75 objective lens. Images were acquired using a Spot Insight digital camera (model 14.2, Color Mosaic; Diagnostic Instruments, Sterling Heights, MI), and were processed with Spotssoftware Advanced (version 4.6 for Windows; Diagnostic Instruments) and Adobe Photoshop version 7.0 software (Adobe Systems, San Jose, CA). (D) Determination of donor origin of the *Bcl11a*-induced leukemia developing in the BMTT-recipient mice. Antibodies staining for CD45.1 or CD45.2 cell-surface molecules were used. (E,F) Determination of cell-lineage origin of the *Bcl11a* leukemia developed in the BMTT-recipient mice. Antibodies against Mac-1, Gr-1, B220, or TCR- β were used to stain lymph nodes and bone marrows harvested from either healthy C57BL/6J mice or mice transplanted with *Bcl11a*-transduced *Nf1*-deficient bone marrow cells to collect evidence for acute myeloid leukemia (E) or T-cell acute lymphoid leukemia (F).

defined by immunophenotyping with antibodies specific for myeloid or lymphoid lineage hematopoietic cells. Antibodies against Mac-1, Gr-1, B220, or TCR- β were used to profile lymph node and bone marrow cells harvested from either healthy C57BL/6J mice or mice transplanted with *Bcl11a*-transduced *Nf1*-deficient bone marrow cells. Although only scarce amounts of Mac-1- and Gr-1-positive cells can be detected in normal lymph node, the number of these cells was increased 11.33-fold plus or minus 4.86-fold in the affected lymph nodes from 5 *Nf1*^(Flox/Fcr).*Bcl11a* mice (Figure 3E), indicating a myeloid lineage of these cells. Similarly, the bone marrow collected from 4 *Nf1*^(Flox/Fcr).*Bcl11a* mice displayed 4.60-fold plus or minus 1.82-fold higher cells staining positive for TCR- β than that harvested from normal mice (Figure 3F), suggesting that these mice have developed T-cell leukemia. Therefore, we conclude that *Bcl11a*-transduced *Nf1*-deficient bone marrow cells cause leukemia in recipient mice, which is derived from transduced donor cells and is of either myeloid or lymphoid lineage.

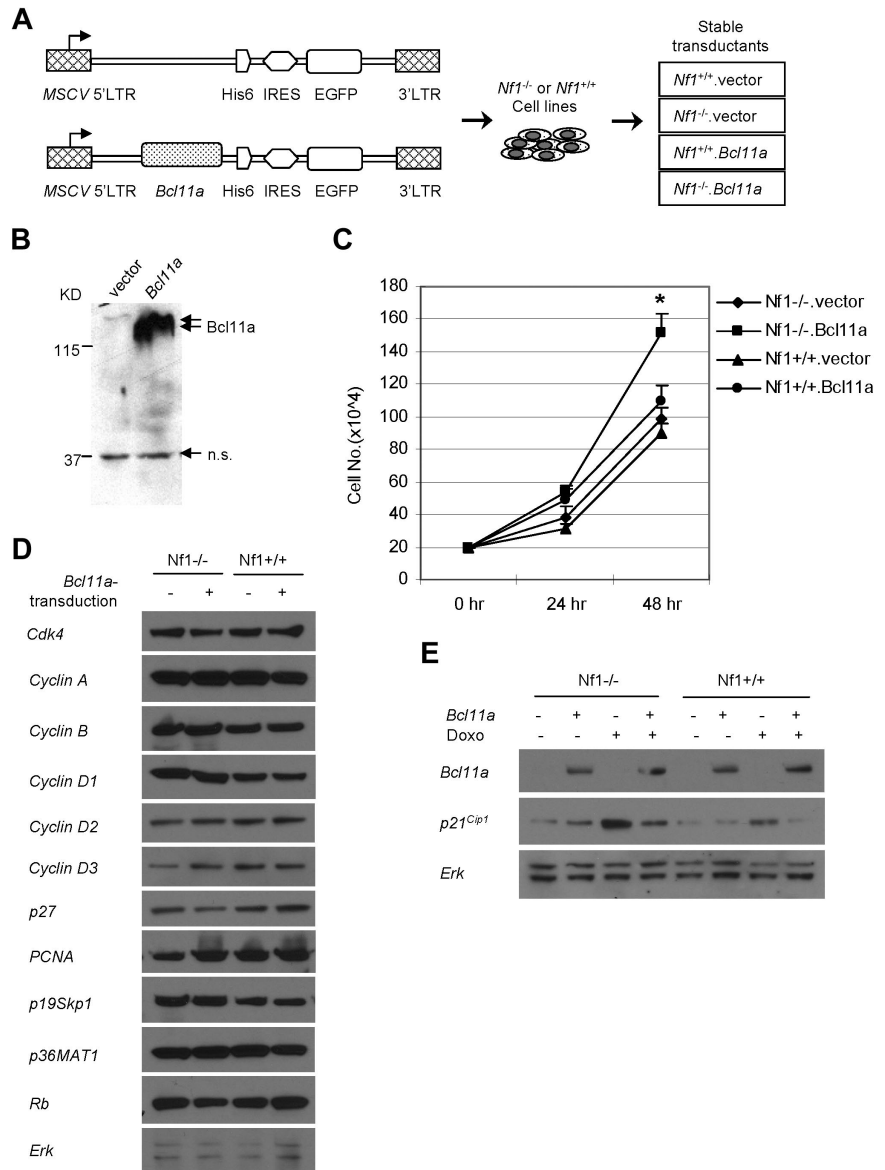
***Bcl11a* down-regulates p21^{Cip1} and promotes *Nf1*-deficient cell growth**

To investigate the mechanism underlying the cooperation between *Bcl11a* and *Nf1* deficiency in leukemogenesis, myeloid cell cultures

with *Bcl11a* overexpression and/or *Nf1* ablation were examined for their growth properties and differentiation potential. Retroviral vectors carrying a His-tagged *Bcl11a* and an EGFP marker, or EGFP alone, were used to transduce *Nf1*-intact or *Nf1*-null Myb-immortalized myeloblast cell line hematopoietic cells¹² (Figure 4A). EGFP-positive cells were then sorted to obtain 4 stably transduced populations: *Nf1*-intact empty vector-transduced cells (*Nf1*^(+/+).vector), *Nf1*-intact *Bcl11a*-transduced cells (*Nf1*^(+/+).*Bcl11a*), *Nf1*-null empty vector-transduced cells (*Nf1*^(-/-).vector), and *Nf1*-null *Bcl11a*-transduced cells (*Nf1*^(-/-).*Bcl11a*). To test functionality of the *Bcl11a*-carrying construct, 293T cells were transiently transfected and subjected to Western blotting assay using anti-His antibody. Abundant *Bcl11a* protein was detected approximately at the position of 170 kDa in *Bcl11a*-transfected cells, but not in vector-transfected cells, indicating specific expression of *Bcl11a* from the retroviral construct (Figure 4B).

After culture for 24 hours, the cumulative cell number of *Nf1*^(-/-).*Bcl11a* cells was only slightly higher than those of 3 other engineered cell lines (Figure 4C). However, this number increased to 1.5-fold those of other cell lines at 48 hours of culture, indicating that *Nf1*^(-/-).*Bcl11a* cells grew significantly faster ($P < .05$) than control cells (Figure 4C). The enhanced growth potential of

Figure 4. *Bcl11a* promotes expansion of an *Nf1*-deficient hematopoietic cell line and *p21^{Cip1}* down-regulation. (A) Scheme for generating *Nf1^{+/+}* or *Nf1^{-/-}* cell lines stably transduced with *Bcl11a*-expressing retroviral construct (*Nf1^{+/+}.Bcl11a* and *Nf1^{-/-}.Bcl11a*) or with empty vector (*Nf1^{+/+}.vector* and *Nf1^{-/-}.vector*) as negative controls. His6 indicates the protein tag of 6 repeats of histidine. (B) Verification of the *Bcl11a*-expressing vector by transient transfection of 293T cells followed by Western blotting assay. Anti-His antibody was used. The double arrows indicate the signal for *Bcl11a*. The single arrow indicates a nonspecific (n.s.) signal. (C) Cumulative growth of the stable *Bcl11a*- or vector-transduced *Nf1^{+/+}* or *Nf1^{-/-}* cells. (D) The abundance of cell-cycle regulatory proteins in stable *Bcl11a* or vector transductants. (E) *p21^{Cip1}* protein level was determined in stable *Bcl11a* or vector transductants after doxorubicin treatment (Doxo) for 16 hours. Representative results from 3 independent experiments were shown here.



Nf1^{-/-}.Bcl11a cells was confirmed by MTS (3-(4,5-dimethylthiazol-2-yl)-5-(3-carboxymethoxyphenyl)-2-(4-sulfophenyl)-2H-tetrazolium, inner salt) assay (data not shown). This result suggests that overexpression of *Bcl11a* can confer a growth advantage to *Nf1*-deficient cells.

To examine the molecular basis of *Bcl11a*-stimulated proliferation advantage, we examined the abundance of cell-cycle regulatory proteins in these cell lines. There were no evident changes between *Nf1* status and/or *Bcl11a* transduction in the basal level of 11 proteins examined, including Cdk4, cyclin A, cyclin B, cyclin D1, cyclin D2, cyclin D3, p27, p21^{Cip1}, PCNA, p19^{Skp1}, p36^{MAT1}, Rb, and Erk (Figure 5D). Interestingly, when challenged for 16 hours with 250 ng/mL doxorubicin, a DNA intercalator and damaging agent, both *Nf1^{-/-}* (Figure 5E lane 3) and *Nf1^{+/+}* (lane 7) cells displayed elevated p21^{Cip1} levels. However, a marked decrease in the induced level of p21^{Cip1} was observed in *Bcl11a*-transduced *Nf1^{-/-}* or *Nf1^{+/+}* cells (lane 4 and lane 8). These results suggest that *Bcl11a* overexpression suppresses elevation of p21^{Cip1} level induced by DNA damage.

Expression of *BCL11A* in human leukemia

To determine whether *BCL11A* could possibly be contributing to human myeloid leukemia, we examined its expression in chronic and acute forms of the disease. *BCL11A* expression levels in JMML and chronic myelomonocytic leukemia were examined by RT-PCR. As can be seen in Figure 6A, *BCL11A* expression is detected in most patient samples from both types of diseases, although lower than detectable in a few samples, which is consistent with the possibility that *BCL11A* expression could make a positive contribution to these diseases. Interestingly, several of the other candidate genes obtained from this insertional mutagenesis screen, including *EDG3*, *MEIS1*, *EKI*, and *DEF8*, were expressed in these diseases (Figure 5A).

A large-scale examination of gene expression in a cohort of 285 patients with AML has been performed using Affymetrix-based microarray.³³ Based on the overall gene expression profile, these patients were grouped into 16 clusters using an unsupervised cluster approach. Of note, 3 sets of *BCL11A*-specific probes all generated comparable hybridization signals across these samples

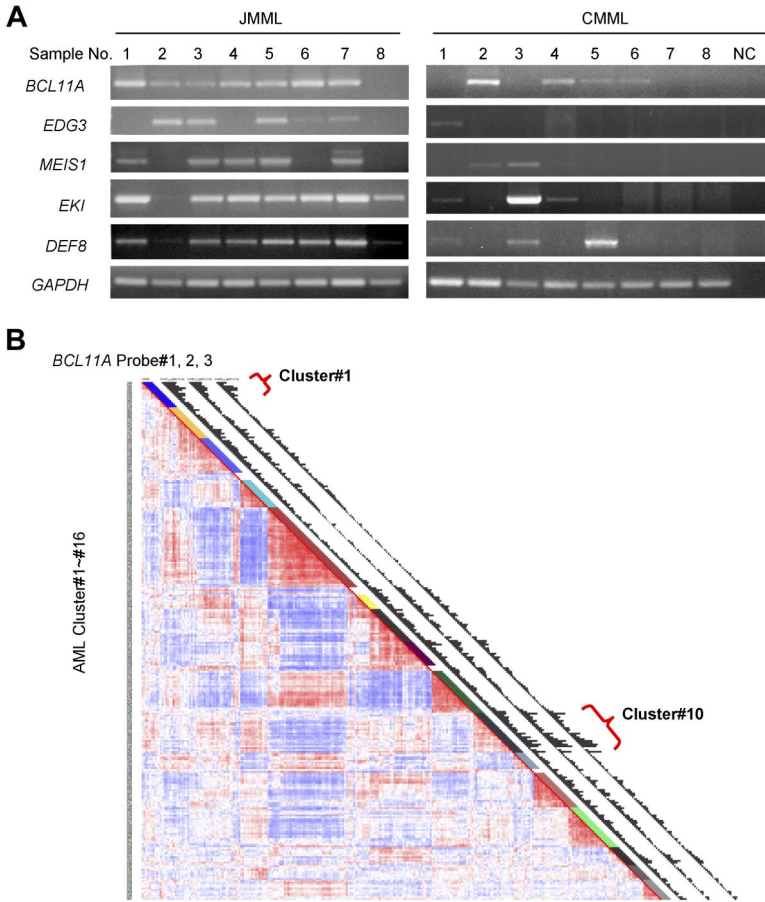


Figure 5. *BCL11A* expression in human leukemia. (A) *BCL11A* expression in human chronic myelomonocytic leukemia and juvenile myelomonocytic leukemia was detected by RT-PCR. NC indicates water in place of cDNA as template for PCR. *GAPDH* was used as a loading control. The JMML samples are found to carry mutations in *KRAS* (no. 1) or *PTPN11* (nos. 2-7), or wild type for both genes (no. 8). (B) Gene expression profiling in a large cohort of human acute myelogenous leukemia. Results using a set of 3 probes for *BCL11A* are displayed. Probe nos. 1, 2, and 3 indicate probe sets, 210347_s_at, 219497_s_at, and 219498_s_at, respectively. Clusters of AML showing increased level of *BCL11A* are noted (clusters 1 and 10).

(Figure 5B). This microarray analysis revealed that *BCL11A* displayed variant abundance of transcripts in AML (Figure 5B). More interestingly, patients with high expression levels of *BCL11A* were mostly segregated into 2 of 16 clusters: cluster 1 and cluster 10 (Figure 6B), whereas other groups and normal bone marrow cells showed low expression of *BCL11A*. Cluster 10 is associated with a poor outcome, and with monosomy 7, which is also common in JMML and in cases of JMML that transform to AML. The association of *BCL11A* level with poor outcome of patients in cluster 10 indicates that *BCL11A* could be up-regulated in this subset of AML and might contribute to these diseases. However, patients in cluster 1 do not show a poor prognosis³³; even many of patients in this group also carry MLL translocations. Genetic complexity of AML and gene expression-based classification of patients could obscure the effects of certain genetic lesions on the

outcome of patients. Other factors, such as monosomy 7 seen in cluster 10, may also contribute to the worse outcome of patients.

Discussion

In this study, we have identified a dozen novel CISs, some of which probably cooperate with *Nf1* deficiency in the development of leukemia. We have, for the first time, demonstrated that *Bcl11a* acts as an oncogene and causes leukemia in the absence of *Nf1* in mice, perhaps through suppression of p21^{Cip1} induction and thereby promotion of cell growth. Our results also suggested that expression of *BCL11A* may contribute to leukemogenesis in certain groups of AML patients.

An association of *BCL11A* with hematologic malignancies has been indicated in the literature. Abnormalities involving *BCL11A* have been detected in a variety of B-cell malignancies in humans.^{14,15,34} The chromosomal region containing the *BCL11A* gene is also recurrently rearranged in other human tumors.³⁵ However, it has been controversial whether *BCL11A* is the real affected gene responsible for the diseases.^{14,34} Furthermore, in 2 of 209 BXH-2 myeloid leukemia, proviral insertion sites were found to be located within the first intron of *Bcl11a* and resulted in increased expression, instead of disruption, of *Bcl11a*.³⁰ *Bcl11a* has also been reported to transform NIH 3T3 in foci formation assay.³⁶ These data support a role of *Bcl11a* as a dominantly acting proto-oncogene. On the other hand, by generating *Bcl11a* knockout mice, Liu et al suggested that *Bcl11a* is critical for B-cell and alpha/beta T-cell development, but not for macrophage-granulocyte and erythroid lineages.¹³

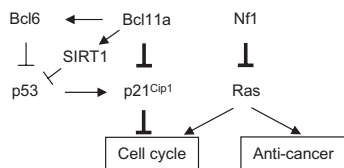


Figure 6. The model for cooperative oncogenesis between *Bcl11a* and *Nf1* deficiency. The thickened lines indicate the major linkage of *Bcl11a*-*Nf1* loss cooperation to leukemogenesis that was identified in this study. The arrows indicate a stimulatory relationship; perpendicular lines, suppression. One major function of *Nf1* is to negatively regulate Ras activity, and *Nf1* deficiency leads to hyperactivation of Ras.^{66,67} Ras activation alone can trigger cell growth arrest and senescence.⁴⁹ However, this effect may be attenuated by an increase in *Bcl11a* signal, which results in suppression of p21^{Cip1} induction and, consequently, release of its control over cell cycle progression, as discovered in this study. *Bcl11a* may directly repress *Cdkn1a* transcription or indirectly through p53 mediated by BCL6^{36,68} or SIRT1.^{64,65,69}

Paradoxically, transplantation of *Bcl11a* knockout mice fetal liver cells resulted in T-cell leukemia originated from recipient mice, suggesting that *Bcl11a* may be a non-cell autonomous T-cell tumor suppressor gene.¹³ Moreover, another member of *Bcl11* family, *Bcl11b*, has been suggested to be a tumor suppressor gene, acting via an increase in resistance to DNA damage.^{37,38} Thus, it has been left unclear whether *Bcl11a* functions as an oncogene or tumor suppressor gene, under what conditions, and in what manner *Bcl11a* can cause tumor.

We found that proviral insertions located downstream of *Bcl11a* concentrated in an *Nf1*-deficient AML panel. Consequently, expression of *Bcl11a* was up-regulated, presumably through long-range activation effect of retroviral insertion.³⁹ Given that no other affected genes around these insertions were identified, these data strongly indicate *Bcl11a* as an oncogene in *Nf1*-deficient myeloid leukemia. Indeed, our findings of the ability of *Bcl11a* overexpression in *Nf1*-deficient bone marrow cells to induce mouse leukemia, combined with our observation of *BCL11A* dysregulation in certain subsets of human AML, have established that *Bcl11a* functions as an oncogene in both myeloid and lymphoid lineages, in a cell autonomous manner, and in the absence of *Nf1* function. These results indicate that *Bcl11a* may have a multilineage effect. The tumorigenicity of an oncogene in multiple cell types has been observed previously.⁴⁰⁻⁴² It is possible, however, that the murine stem cell virus–long terminal repeat used to express *Bcl11a* in our study could create a bias toward T-cell malignancy.^{43,44} Transgenic models using different promoters to express *Bcl11a* would provide a different approach to look at the lineage tropism of *Bcl11a* oncogenicity. Our study also suggests whether *Bcl11a* is implicated in human neoplasias other than lymphoid diseases will need to be examined.

There are indications that secondary genetic events are needed for the development of leukemia initiated by *Nf1* deficiency. Although the cooperation of *Nf1* deficiency with other genetic alterations has been proposed or attempted,^{29,45,46} convincing evidence is still lacking. Our results suggest the existence of a strong synergetic effect of *Bcl11a* up-regulation and *Nf1* deficiency. This cooperation has not been revealed by any other kind of PIS studies, including a recent extensive computational analysis of PISs deposited in the Retrovirus Tagged Cancer Gene Database.⁴⁷ Recent studies suggested that defects in DNA repair genes influence *NF1* tumor progression in mice and humans, presumably by inactivating normal allele of *NF1*.^{46,48} We found that formation of leukemia with *Nf1* biallelic inactivation and *Bcl11a* overexpression was markedly accelerated, suggesting that other genetic lesions may contribute more significantly to the observed progression of *NF1* tumor than loss of heterozygosity of *NF1*. In addition, myeloproliferative disorder (MPD) can progress to AML; however, there are no solid experimental data explaining the progression of MPD into AML in the context of JMML or other *NF1*-associated myeloid diseases. It has been shown that mice with *Nf1* deficiency in hematopoietic cells develop an MPD-like disease.^{11,12,32} Based on these studies, our genetic study has provided a mouse model, clearly demonstrating that *Nf1*-associated MPD, on acquisition of *Bcl11a* dysregulation, is capable of progression into AML.

Combined with previously published work, we propose a model of our current understanding of the *Bcl11a/Nf1* deficiency cooperation. Dysregulated Ras signaling has been the only known major downstream effect of *Nf1* deficiency in cancer so far. Ras activation alone in primary fibroblasts could trigger p53/p16-dependent growth arrest and senescence.⁴⁹ These cell-defensive responses, however, during the development of leukemia could be overcome through the acquired enhancement of *Bcl11a* expression, which could result in suppression of p21^{Cip1}

induction. The role of p21^{Cip1} in multiple aspects of hematopoiesis has been documented.⁵⁰⁻⁵⁹ p21^{Cip1} induction is correlated with reduced colony formation and cell-cycle arrest of hematopoietic progenitor cells or leukemic cells.⁵⁰⁻⁵³ p21^{Cip1} loss cooperates with *AML1-ETO* in leukemogenesis and accelerates the onset of mouse mammary tumor virus H-ras-induced tumors.^{59,60} Interestingly, N-ras oncogene up-regulates p21^{Cip1} in hematopoietic cells, but Ras does not induce growth arrest in p21^{Cip1}-null fibroblasts, and p21^{Cip1} loss can rescue Ras-driven anchorage independence and tumorigenesis.^{56,61,62} The p21^{Cip1} suppression by *Bcl11a* could be as a result of direct repression of *Cdkn1a* transcription by *Bcl11a*. We have noticed that the *Cdkn1a* gene has 2 potential *Bcl11a*-binding sites in its promoter region, which supports the assumption of direct mode of suppression. An experimental validation of *Cdkn1a* as a direct transcriptional target of *Bcl11a* is warranted. The suppressive effect of *Bcl11a* could also be exerted indirectly through other intermediate proteins.^{36,63-65} Thus, it is probable that *Nf1* deficiency in hematopoietic cells may cause the similar effects as Ras activation, which requires cooperation with other genetic abnormalities, such as *Bcl11a* overexpression, to develop further into aggressive forms of leukemia.

We expect that the establishment of *Bcl11a*'s oncogenic role will stimulate further understanding of its biologic function and molecular mechanisms in disorders and eventually allow for the development of therapeutic strategies in the treatment of *Bcl11a*-relevant diseases.

Acknowledgments

We thank Ms Jennifer Jeske-Geurts and Ms Raha Allaei for breeding and genotyping mice, Ms Miechaleen Diers for mouse tail vein injection, Dr Sheri Kuslak for cloning assistance, Dr Xianghua Luo from the Biostatistics Core of the University of Minnesota Cancer Center for help with statistical analyses, the Histopathology Core of the University of Minnesota Cancer Center for tissue sectioning and pathologic examination, the Flow Cytometry Core of the University of Minnesota Cancer Center for assistance in immunophenotyping murine leukemia, Dr Jessica Walrath and Dr Susan Blaydes Ingersoll for providing genomic DNA derived from *Nf1*-deficient BXH-2 mice, and Dr Luis Parada for providing *Nf1* conditional knockout mice and Leukemia & Lymphoma Society of America (LLS 7019-04).

This work was supported by the National Institutes of Health (grant CA84221) and Leukemia & Lymphoma Society of America (LLS 7019-04).

Authorship

Contribution: B.Y. designed, performed, collected, analyzed, and interpreted experimental data, and wrote the manuscript; R.D. and P.J.V. performed research and collected data; M.R.W. and M.L.L. contributed vital new reagents; K.M.S. oversaw the direction of all experimental studies and edited the manuscript; and D.A.L. oversaw the direction of all experimental studies, designed research, evaluated the data, and edited the manuscript.

Conflict-of-interest disclosure: The authors declare no competing financial interests.

Correspondence: David A. Largaespada, University of Minnesota, 6-160 Jackson Hall, 321 Church Street SE, Minneapolis, MN 55455; e-mail: larga002@tc.umn.edu.

References

- Arun D, Gutmann DH. Recent advances in neurofibromatosis type 1. *Curr Opin Neurol*. 2004;17:101-105.
- Martin GA, Viskochil D, Bollag G, et al. The GAP-related domain of the neurofibromatosis type 1 gene product interacts with ras p21. *Cell*. 1990;63:843-849.
- DeClue JE, Papageorge AG, Fletcher JA, et al. Abnormal regulation of mammalian p21ras contributes to malignant tumor growth in von Recklinghausen (type 1) neurofibromatosis. *Cell*. 1992;69:265-273.
- Basu TN, Gutmann DH, Fletcher JA, Glover TW, Collins FS, Downward J. Aberrant regulation of ras proteins in malignant tumour cells from type 1 neurofibromatosis patients. *Nature*. 1992;356:713-715.
- Johnson MR, Look AT, DeClue JE, Valentine MB, Lowy DR. Inactivation of the NF1 gene in human melanoma and neuroblastoma cell lines without impaired regulation of GTP Ras. *Proc Natl Acad Sci U S A*. 1993;90:5539-5543.
- Guo HF, The I, Hannan F, Bernards A, Zhong Y. Requirement of Drosophila NF1 for activation of adenylyl cyclase by PACAP38-like neuropeptides. *Science*. 1997;276:795-798.
- Tong JJ, Schriener SE, McCleary D, Day BJ, Wallace DC. Life extension through neurofibromin mitochondrial regulation and antioxidant therapy for neurofibromatosis-1 in *Drosophila melanogaster*. *Nat Genet*. 2007;39:476-485.
- Xu H, Gutmann DH. Mutations in the GAP-related domain impair the ability of neurofibromin to associate with microtubules. *Brain Res*. 1997;759:149-152.
- Stiller CA, Chessells JM, Fitchett M. Neurofibromatosis and childhood leukaemia/lymphoma: a population-based UKCCSG study. *Br J Cancer*. 1994;70:969-972.
- Shannon KM, Le Beau MM, Largaespada DA, Killeen N. Modeling myeloid leukemia tumor suppressor gene inactivation in the mouse. *Semin Cancer Biol*. 2001;11:191-200.
- Zhang Y, Taylor BR, Shannon K, Clapp DW. Quantitative effects of Nf1 inactivation on in vivo hematopoiesis. *J Clin Invest*. 2001;108:709-715.
- Largaespada DA, Brannan CI, Jenkins NA, Copeland NG. Nf1 deficiency causes Ras-mediated granulocyte/macrophage colony stimulating factor hypersensitivity and chronic myeloid leukemia. *Nat Genet*. 1996;12:137-143.
- Liu P, Keller JR, Ortiz M, et al. Bcl11a is essential for normal lymphoid development. *Nat Immunol*. 2003;4:525-532.
- Satterwhite E, Sonoki T, Willis TG, et al. The BCL11 gene family: involvement of BCL11A in lymphoid malignancies. *Blood*. 2001;98:3413-3420.
- Weniger MA, Pulford K, Gesk S, et al. Gains of the proto-oncogene BCL11A and nuclear accumulation of BCL11A(XL) protein are frequent in primary mediastinal B-cell lymphoma. *Leukemia*. 2006;20:1880-1882.
- Saiki Y, Yamazaki Y, Yoshida M, Katoh O, Nakamura T. Human EVI9, a homologue of the mouse myeloid leukemia gene, is expressed in the hematopoietic progenitors and down-regulated during myeloid differentiation of HL60 cells. *Genomics*. 2000;70:387-391.
- Jenkins NA, Copeland NG, Taylor BA, Bedigian HG, Lee BK. Ecotropic murine leukemia virus DNA content of normal and lymphomatous tissues of BXH-2 recombinant inbred mice. *J Virol*. 1982;42:379-388.
- Buchberg AM, Bedigian HG, Jenkins NA, Copeland NG. Evi-2, a common integration site involved in murine myeloid leukemogenesis. *Mol Cell Biol*. 1990;10:4658-4666.
- Largaespada DA, Shaughnessy JD Jr, Jenkins NA, Copeland NG. Retroviral integration at the Evi-2 locus in BXH-2 myeloid leukemia cell lines disrupts Nf1 expression without changes in steady-state Ras-GTP levels. *J Virol*. 1995;69:5095-5102.
- Yin B, Kogan SC, Dickins RA, Lowe SW, Largaespada DA. Trp53 loss during in vitro selection contributes to acquired Ara-C resistance in acute myeloid leukemia. *Exp Hematol*. 2006;34:631-641.
- Yin B, Morgan K, Hasz DE, Mao Z, Largaespada DA. Nf1 gene inactivation in acute myeloid leukemia cells confers cytarabine resistance through MAPK and mTOR pathways. *Leukemia*. 2006;20:151-154.
- Brannan CI, Perkins AS, Vogel KS, et al. Targeted disruption of the neurofibromatosis type-1 gene leads to developmental abnormalities in heart and various neural crest-derived tissues. *Genes Dev*. 1994;8:1019-1029.
- Zhu Y, Romero MI, Ghosh P, et al. Ablation of NF1 function in neurons induces abnormal development of cerebral cortex and reactive gliosis in the brain. *Genes Dev*. 2001;15:859-876.
- Yin B, Largaespada DA. PCR-based procedures to isolate insertion sites of DNA elements. *Bio-techniques*. 2007;43:79-84.
- Altschul SF, Madden TL, Schaffer AA, et al. Gapped BLAST and PSI-BLAST: a new generation of protein database search programs. *Nucleic Acids Res*. 1997;25:3389-3402.
- Yin B, Tsai ML, Hasz DE, Rathe SK, Le Beau MM, Largaespada DA. A microarray study of altered gene expression after cytarabine resistance in acute myeloid leukemia. *Leukemia*. 2007;21:1093-1097.
- Sohal J, Phan VT, Chan PV, et al. A model of APL with FLT3 mutation is responsive to retinoic acid and a receptor tyrosine kinase inhibitor, SU11657. *Blood*. 2003;101:3188-3197.
- Attygalle A, Al-Jehani R, Diss TC, et al. Neoplastic T cells in angioimmunoblastic T-cell lymphoma express CD10. *Blood*. 2002;99:627-633.
- Blaydes SM, Kogan SC, Truong BT, et al. Retroviral integration at the Epi1 locus cooperates with Nf1 gene loss in the progression to acute myeloid leukemia. *J Virol*. 2001;75:9427-9434.
- Nakamura T, Largaespada DA, Shaughnessy JD Jr, Jenkins NA, Copeland NG. Cooperative activation of Hoxa and Pbx1-related genes in murine myeloid leukaemias. *Nat Genet*. 1996;12:149-153.
- Wakioka T, Sasaki A, Kato R, et al. Spred is a Sprouty-related suppressor of Ras signalling. *Nature*. 2001;412:647-651.
- Le DT, Kong N, Zhu Y, et al. Somatic inactivation of Nf1 in hematopoietic cells results in a progressive myeloproliferative disorder. *Blood*. 2004;103:4243-4250.
- Valk PJ, Verhaak RG, Beijten MA, et al. Prognostically useful gene-expression profiles in acute myeloid leukemia. *N Engl J Med*. 2004;350:1617-1628.
- Martin-Subero JI, Gesk S, Harder L, et al. Recurrent involvement of the REL and BCL11A loci in classical Hodgkin lymphoma. *Blood*. 2002;99:1474-1477.
- Mitelman F, Johansson B, Mertens F (eds). *Mitelman Database of Chromosome Aberrations in Cancer*. <http://cgap.ncinihgov/Chromosomes/Mitelman>. Accessed July 18, 2007.
- Nakamura T, Yamazaki Y, Saiki Y, et al. Evi9 encodes a novel zinc finger protein that physically interacts with BCL6, a known human B-cell proto-oncogene product. *Mol Cell Biol*. 2000;20:3178-3186.
- Kamimura K, Mishima Y, Obata M, Endo T, Aoyagi Y, Kominami R. Lack of Bcl11b tumor suppressor results in vulnerability to DNA replication stress and damages. *Oncogene*. 2007;26:5840-5850.
- Kamimura K, Ohi H, Kubota T, et al. Haploinsufficiency of Bcl11b for suppression of lymphomagenesis and thymocyte development. *Biochem Biophys Res Commun*. 2007;355:538-542.
- Hanlon L, Barr NI, Blyth K, et al. Long-range effects of retroviral insertion on c-myc: overexpression may be obscured by silencing during tumor growth in vitro. *J Virol*. 2003;77:1059-1068.
- Weinberg RA. *The Biology of Cancer*. 1st ed. Oxford, United Kingdom: Garland Science; 2006.
- Voncken JW, Kaartinen V, Pattengale PK, Germeraad WT, Groffen J, Heisterkamp N. BCR/ABL P210 and P190 cause distinct leukemia in transgenic mice. *Blood*. 1995;86:4603-4611.
- Heisterkamp N, Jenster G, ten Hoeve J, Zovich D, Pattengale PK, Groffen J. Acute leukaemia in bcr/abl transgenic mice. *Nature*. 1990;344:251-253.
- Dedera DA, Waller EK, LeBrun DP, et al. Chimeric homeobox gene E2A-Pbx1 induces proliferation, apoptosis, and malignant lymphomas in transgenic mice. *Cell*. 1993;74:833-843.
- Kamps MP, Baltimore D. E2A-Pbx1, the t(1;19) translocation protein of human pre-B-cell acute lymphocytic leukemia, causes acute myeloid leukemia in mice. *Mol Cell Biol*. 1993;13:351-357.
- King D, Yang G, Thompson MA, Hiebert SW. Loss of neurofibromatosis-1 and p19(Arf) cooperate to induce a multiple tumor phenotype. *Oncogene*. 2002;21:4978-4982.
- Gutmann DH, Winkler E, Kabbarah O, et al. Mlh1 deficiency accelerates myeloid leukemogenesis in neurofibromatosis 1 (Nf1) heterozygous mice. *Oncogene*. 2003;22:4581-4585.
- de Ridder J, Kool J, Uren A, Bot J, Wessels L, Reinders M. Co-occurrence analysis of insertional mutagenesis data reveals cooperating oncogenes. *Bioinformatics*. 2007;23:133-141.
- Bandipalliam P. Syndrome of early onset colon cancers, hematologic malignancies & features of neurofibromatosis in HNPCC families with homozygous mismatch repair gene mutations. *Fam Cancer*. 2005;4:323-333.
- Serrano M, Lin AW, McCurrach ME, Beach D, Lowe SW. Oncogenic ras provokes premature cell senescence associated with accumulation of p53 and p16INK4a. *Cell*. 1997;88:593-602.
- Schmelz K, Wagner M, Dorken B, Tamm I. 5-Aza-2'-deoxycytidine induces p21WAF expression by demethylation of p73 leading to p53-independent apoptosis in myeloid leukemia. *Int J Cancer*. 2005;114:683-695.
- Yoon BI, Hirabayashi Y, Kawasaki Y, et al. Mechanism of action of benzene toxicity: cell cycle suppression in hemopoietic progenitor cells (CFU-GM). *Exp Hematol*. 2001;29:278-285.
- Steinman RA, Yaroslavskiy B, Kaplan SS, Goff JP, Shields DS. Clonal response of K562 leukemia cells to exogenous p21WAF1. *Leuk Res*. 2000;24:601-610.
- Baccini V, Roy L, Vitrat N, et al. Role of p21(Cip1/Waf1) in cell-cycle exit of endomitotic megakaryocytes. *Blood*. 2001;98:3274-3282.
- Albanese P, Chagraoui J, Charon M, et al. Forced expression of p21 in G1Ib-p21 transgenic mice induces abnormalities in the proliferation of erythroid and megakaryocyte progenitors and primitive hematopoietic cells. *Exp Hematol*. 2002;30:1263-1272.
- Alcantara O, Boldt DH. Iron deprivation blocks multilineage haematopoietic differentiation by inhibiting induction of p21(WAF1/CIP1). *Br J Haematol*. 2007;137:252-261.
- Shen S, Passioura T, Symonds G, Dolnikov A.

- N-ras oncogene-induced gene expression in human hematopoietic progenitor cells: upregulation of p16INK4a and p21CIP1/WAF1 correlates with myeloid differentiation. *Exp Hematol*. 2007;35:908-919.
57. Mantel C, Luo Z, Canfield J, Braun S, Deng C, Broxmeyer HE. Involvement of p21cip-1 and p27kip-1 in the molecular mechanisms of steel factor-induced proliferative synergy in vitro and of p21cip-1 in the maintenance of stem/progenitor cells in vivo. *Blood*. 1996;88:3710-3719.
58. Cheng T, Rodrigues N, Shen H, et al. Hematopoietic stem cell quiescence maintained by p21cip1/waf1. *Science*. 2000;287:1804-1808.
59. Peterson LF, Yan M, Zhang DE. The p21Waf1 pathway is involved in blocking leukemogenesis by the t(8;21) fusion protein AML1-ETO. *Blood*. 2007;109:4392-4398.
60. Jackson RJ, Adnane J, Coppola D, Cantor A, Sebtli SM, Pledger WJ. Loss of the cell cycle inhibitors p21(Cip1) and p27(Kip1) enhances tumorigenesis in knockout mouse models. *Oncogene*. 2002;21:8486-8497.
61. Wei W, Jobling WA, Chen W, Hahn WC, Sedivy JM. Abolition of cyclin-dependent kinase inhibitor p16Ink4a and p21Cip1/Waf1 functions permits Ras-induced anchorage-independent growth in telomerase-immortalized human fibroblasts. *Mol Cell Biol*. 2003;23:2859-2870.
62. Oskarsson T, Essers MA, Dubois N, et al. Skin epidermis lacking the c-Myc gene is resistant to Ras-driven tumorigenesis but can reacquire sensitivity upon additional loss of the p21Cip1 gene. *Genes Dev*. 2006;20:2024-2029.
63. Sherr CJ. Divorcing ARF and p53: an unsettled case. *Nat Rev Cancer*. 2006;6:663-673.
64. Senawong T, Peterson VJ, Leid M. BCL11A-dependent recruitment of SIRT1 to a promoter template in mammalian cells results in histone deacetylation and transcriptional repression. *Arch Biochem Biophys*. 2005;434:316-325.
65. Luo J, Nikolaev AY, Imai S, et al. Negative control of p53 by Sir2alpha promotes cell survival under stress. *Cell*. 2001;107:137-148.
66. Khalaf WF, Yang FC, Chen S, et al. K-ras is critical for modulating multiple c-kit-mediated cellular functions in wild-type and *Nf1*^{+/-} mast cells. *J Immunol*. 2007;178:2527-2534.
67. Kim A, Morgan K, Hasz DE, et al. Beta common receptor inactivation attenuates myeloproliferative disease in *Nf1* mutant mice. *Blood*. 2007;109:1687-1691.
68. Phan RT, Dalla-Favera R. The BCL6 proto-oncogene suppresses p53 expression in germinal-centre B cells. *Nature*. 2004;432:635-639.
69. Langley E, Pearson M, Faretta M, et al. Human SIR2 deacetylates p53 and antagonizes PML/p53-induced cellular senescence. *EMBO J*. 2002;21:2383-2396.